Governing soliton splitting in one-dimensional lattices

Andrea Fratalocchi* and Gaetano Assanto†
Nonlinear Optics and OptoElectronics Labs (NooEL), National Institute for the Physics of Matter (INFM), and CNISM, Department of Electronic Engineering, University Roma, Tre Via della Vasca Navale 84, 00146, Rome, Italy
(Received 6 July 2005; published 7 April 2006)

We investigate discrete light dynamics in the presence of a longitudinal defect of arbitrary extension, amplitude and position in a nonlinear waveguide array. We model and discuss the physics of the soliton-defect interaction, showing how to gain complete control over the system outcome for soliton-based data processing. We propose all-optical management in dye-doped liquid crystals.

DOI: 10.1103/PhysRevE.73.046603 PACS number(s): 42.65.Tg, 42.70.Df, 42.65.Jx

I. INTRODUCTION

Energy localization in the presence of discreteness has gained importance in several branches of contemporary science, including—but not limited to—biological systems [1], nonlinear optics [2], Bose-Einstein condensates (BECs) [3], and solid state physics [4]. Considerable attention has been devoted to systems with tunable lattice parameters, such as arrays of waveguides in photorefractives [5,6] or nematic liquid crystals (NLCs) [7], or BEC droplets [3,8]. The electro-optic response of NLCs and photorefractives allows to tune the lattice linear properties (refractive modulation) [5–7], whereas Feshbach-resonance can modulate and reverse the nonlinearity in the BEC [9]. In fact, significant advancements in soliton-based data processing (SDP) [5,10] can be foreseen in those geometries and/or materials where nonlinearity can be tuned and hence light dynamics controlled.

A promising and powerful approach to the latter aim is the interaction between solitons (or, more generally, solitary waves or transversely localized light) and defects. The study of such interactions is of great importance [11–16] and can be generalized to nonlinear waveguides of arbitrary physical nature [17]. Despite some previous attempts in specific cases [13] and transverse inhomogeneities [11,12,14–16], however, a thorough analysis of soliton-defect interactions in the relevant case of defects (localized or extended) encountered during propagation was not carried out before to our knowledge. While in the case of linear inhomogeneities numerical and theoretical studies demonstrated that a defect may reflect, transmit, or trap the soliton around it [11,12,14–16], for nonlinear infinitesimal defects numerical simulations showed that a soliton may split into secondary pulses if the perturbation exceeds a threshold [13]. A similar dynamics was observed in discrete and continuous systems with periodic transverse properties [9,18–20]. However, the physics of the latter type of interaction is not clear to date, as its comprehension was limited to numerical approaches to the problem [9,13,18–20].

In this paper we investigate discrete light dynamics in the case of an arbitrary longitudinal defect located in a specific section of a waveguide array, perpendicular to the waveguide axes. With reference to a dielectric array, but undertaking a general approach (which also applies to the continuum) [21], we model soliton-defect interactions and unveil the underlying physics (Secs. II and III). It is well known that a discrete array is governed by a nonintegrable model; therefore, to provide analytical results, we first focus on the long-wavelength limit [21]. We introduce an original approach to achieve full control over the system, anticipating a series of potential applications to SDP. Light-reconfigurable all-optical circuits can be envisioned where data are coded into guided light signals and manipulated by illuminating a region of the nonlinear array, a concept amenable to find applications in various media. Finally, we propose a viable implementation in doped NLC arrays [22–24], as they exhibit excellent potentials for nonlinear optics while also being electro-optically adjustable [7].

II. THEORETICAL MODEL

Discrete light propagation can be described by a discrete nonlinear Schrödinger equation (DNLSE) [1–4,25]. In the presence of a single nonlinear defect, the DNLSE can be cast in the form

$$i\frac{\partial q_n}{\partial Z} + (q_{n+1} + q_{n-1} - 2q_n) + 2[1 + R(Z)]q_n|q_n|^2 = 0 \quad (1)$$

q_n being a dimensionless slowly varying mode envelope [2] (or wave function for BEC or molecular systems [1–3]), Z a normalized propagation coordinate, and $R(Z)=\frac{\delta}{2\Delta}\mathrm{rect}\left(\frac{Z-Z_0}{\Delta}\right)$ the contribution arising from a uniform nonlinear defect with δ, Δ, and Z_0 arbitrary constants.The long-wavelength (quasi-continuum [26]) limit of Eq. (1) is obtained by replacing n with the continuous variable X and expanding the linear terms $q_{n\pm1}$ in a Taylor series around $X=n$, i.e.,

$$i\frac{\partial \psi}{\partial Z} + \frac{\partial^2 \psi}{\partial X^2} + 2(1 + R)|\psi|^2\psi = 0 \quad (2)$$

where we set $\psi(X,Z)=q_n(Z)$. Equation (2) is a perturbed version of the nonlinear Schrödinger equation, which can be regarded as a general model of dispersive nonlinear media [27,28]. To investigate the evolution of a high-order soliton pulse of the type $\psi(X,0)=nA\,\mathrm{sech}(AX)$, with arbitrary n and

*Electronic address: frataloc@uniroma3.it
†Electronic address: assanto@uniroma3.it

A, we address the two limits $\Delta \ll 1$ and $\Delta \gg 1$ and then discuss the intermediate cases.

A. Soliton splitting in δ-like defects

1. Model and solution

When Δ is smaller than any characteristic soliton length, the defect can be described by $R(Z)=\frac{\delta}{2}u_0(Z-Z_0)$, with u_0 the Dirac δ function. The outgoing wave ψ_+ at $Z=Z_{0+}$ can be obtained by integrating Eq. (2). This gives $\psi_+ = \psi_- \exp(i\delta|\psi_-|^2)$, ψ_- being the incoming wave at $Z=Z_{0-}$. The emerging solution is completely characterized by the Zakharov-Shabat (ZS) non-self-adjoint eigenvalue problem [29,30]

$$i\frac{\partial \mathbf{v}}{\partial X} + \mathbf{U}\mathbf{v} - \zeta\sigma_3\mathbf{v} = \mathbf{0}, \quad \mathbf{U} = \begin{bmatrix} 0 & q \\ q^* & 0 \end{bmatrix}, \tag{3}$$

where $\mathbf{v}=[v_1(X), v_2(X)]$, $q(X)=\psi(X, Z_{0+})$ is the scattering potential, and σ_3 the Pauli spin matrix [30]. The amplitude and phase of the emerging solitons are proportional to imaginary and real parts of the discrete eigenvalues ζ_m, respectively, corresponding to the discrete spectrum of the scattering data [29].

We aim at relating the splitting onset in δ to the input parameters A and n. Equation (2) is invariant under the scaling $X \to \alpha X$, $Z \to \alpha^2 Z$, $\psi \to \frac{\psi}{\alpha}$, and $\delta \to \delta\alpha^2$, with α an arbitrary constant. Without loss of generality, we can take real the amplitude A and $nA \geqslant 2$ for integers $n \geqslant 1$; owing to the symmetries of Eqs. (3) [30], we focus on positive δ. With the introduction of an arbitrarily small parameter $\epsilon=(An)^{-1}$, the scattering potential q of the ZS eigenvalue problem becomes $q=\frac{P(X)}{\epsilon}\exp\left(i\frac{Q(X)}{\epsilon^2}\right)$ with $P(X)=\mathrm{sech}(AX)$ and $Q(X)=\delta|\mathrm{sech}(AX)|^2$. By the change of variables

$$v_1 = s_1(Y)\exp\left(i\frac{Q}{2\epsilon^2}\right),$$

$$v_2 = s_2(Y)\exp\left(-i\frac{Q}{2\epsilon^2}\right), \tag{4}$$

with $Y=X\epsilon$, $Q \to Q(Y)$, and $P \to P(Y)$, we can recast Eq. (3) as a coupled Schrödinger-like problem with complex potentials:

$$4\epsilon^4\begin{bmatrix} \frac{\partial^2 s_1}{\partial Y^2} \\ \frac{\partial^2 s_2}{\partial Y^2} \end{bmatrix} = \begin{bmatrix} -4|P(Y)|^2 - \left(2\lambda + \frac{\partial Q}{\partial Y}\right)^2 - 2i\epsilon^2\frac{\partial^2 Q}{\partial Y^2} & i4\epsilon^2\frac{\partial P}{\partial Y} \\ i4\epsilon^2\frac{\partial P}{\partial Y} & -4|P(Y)|^2 - \left(2\lambda + \frac{\partial Q}{\partial Y}\right)^2 + 2i\epsilon^2\frac{\partial^2 Q}{\partial Y^2} \end{bmatrix}\begin{bmatrix} s_1(Y) \\ s_2(Y) \end{bmatrix} \tag{5}$$

with $\lambda=\zeta\epsilon^2$ and $V_{\mathrm{eff}}=-|P|^2-(\partial_Y Q/2)^2$ its effective potential. When the phase amplitude δ is small, V_{eff} has a single minimum in $X=0$ and the eigenfunctions corresponding to the low-energy states inside the potential well (or equivalently with a large imaginary eigenvalue η in the ZS scattering problem) are localized near this point [31]. In this configuration the effect of the imaginary term $2i\epsilon^2\frac{\partial^2 Q}{\partial Y^2}$ can be neglected as long as $\delta=O(\epsilon)$ ($Q \propto \delta$). The remaining system (5) can be diagonalized by

$$\begin{bmatrix} s_1 \\ s_2 \end{bmatrix} = \begin{bmatrix} -1 & 1 \\ 1 & 1 \end{bmatrix}\begin{bmatrix} w_1 \\ w_2 \end{bmatrix}, \tag{6}$$

obtaining two independent Schrödinger-like problems:

$$4\epsilon^4\begin{bmatrix} \frac{\partial^2 w_1}{\partial Y^2} \\ \frac{\partial^2 w_2}{\partial Y^2} \end{bmatrix} = \begin{bmatrix} -4|P(Y)|^2 - \left(2\lambda + \frac{\partial Q}{\partial Y}\right)^2 - 4i\epsilon^2\frac{\partial P}{\partial Y} & 0 \\ 0 & -4|P(Y)|^2 - \left(2\lambda + \frac{\partial Q}{\partial Y}\right)^2 + 4i\epsilon^2\frac{\partial P}{\partial Y} \end{bmatrix}\begin{bmatrix} w_1(Y) \\ w_2(Y) \end{bmatrix}. \tag{7}$$

Then we perform a series expansion of P and Q near the effective potential minimum, by introducing $|P(Y)|^2=P_0 - P_2Y^2+O(Y^3)$, $\partial_Y Q(Y)=Q_1Y+O(Y^2)$, and $Y_1=\epsilon^2 Y$ thus obtaining [up to order $O(\epsilon^4)$] the normalized eigenvalue equation for the quantum harmonic oscillator [32]:

$$\frac{\partial^2 w_{1,2}}{\partial T^2} + (\sigma - T^2)w_{1,2} = 0 \tag{8}$$

with $\lambda_1=i\lambda$, $\gamma=4P_2-Q_1^2$ and for w_1,

$$Y_1 = \frac{\sqrt{\gamma}\epsilon^2}{2}T - i\frac{2(2P_2 + Q_1\lambda_1/\epsilon^2)}{\gamma},$$

$$\sigma = \frac{2P_0\gamma - 2[\ \gamma\lambda_1 + (-2P_2\epsilon^2 + Q_1\lambda_1)^2)]}{\gamma\sqrt{\gamma}\epsilon^2},$$

and for w_2,

$$Y_1 = -\frac{\sqrt{\gamma}\epsilon^2}{2}T + i\frac{2(2P_2 + Q_1\lambda_1/\epsilon^2)}{\gamma},$$

$$\sigma = \frac{2P_0\gamma - 2[\ \gamma\lambda_1 + (2P_2\epsilon^2 + Q_1\lambda_1)^2)]}{\gamma\sqrt{\gamma}\epsilon^2}. \tag{9}$$

The first two excited eigenvalues λ_{1a} and λ_{1b} (solutions for $\sigma=1$) are real for $Q_1=0$, therefore the eigenvalues ζ_m and the coordinate shifts (9) are purely imaginary. Hence, the soliton configuration is stable in $Y=0$. The distance between λ_{1a} and λ_{1b} decreases as Q_1 grows and goes to zero when $\gamma=0$. Following the eigenvalue collision, the effective potential V_{eff} undergoes a classical cusp catastrophe [33,34], i.e., two new minima $Y_\pm$ are created and $Y=0$ becomes a local maximum. The symmetry of the eigenfunctions localized around $Y=X=0$ is broken; a Taylor expansion around the new minima reveals a nontrivial real part of the eigenvalue [arising from $\partial_Y Q(Y_\pm)$ with different signs for $Y_\pm$]. The critical δ_c, providing a symmetry-breaking perturbation of the ground-state eigenfunctions, corresponds to $\gamma=0$ and is $\delta_c=\frac{1}{nA^2}$. The latter expression is $O(\epsilon)$ and, therefore, our initial assumption is justified. For a fixed A, such that $\epsilon=(An)^{-1}<1$, the distribution δ_c versus n is found by defining $\delta_n=\delta_c(n)$ and iterating $\delta_{n+1}=\frac{n}{n+1}\delta_n$, a dissipative one-dimensional (1D) map with a damping factor $0.5\leqslant\frac{n}{n+1}<1$ [35]. For a variable A, the starting point in the plane (δ_n,δ_{n+1}) is always attracted toward the stable fixed point in the origin for increasing n. To verify this result, we numerically solve the ZS problem (3) and evaluate δ_c for various solitary input parameters (Fig. 1). As predicted, when the soliton number n increases, δ_c rapidly tends to the fixed point (0,0), independently from the initial position in (δ_n,δ_{n+1}) and in excellent agreement with the asymptotic dependence (dotted lines in Fig. 1).

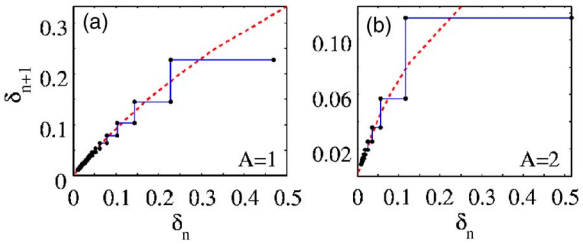

FIG. 1. (Color online) Theoretical (dashed line) and numerical (dots) critical phase amplitude $\delta_c(n)$ in the plane (δ_n,δ_{n+1}) for $A=1$ and $2\leqslant n\leqslant 20$ (a), $A=2$ and $1\leqslant n\leqslant 20$ (b).

2. Tuning the bifurcation onset and all-optical soliton generation

Since δ_c decreases as the beam amplitude An increases (for $Z_0=0$), an interesting splitting scenario is expected for $Z_0\neq 0$ and amplitude or waist modulated (i.e., breathing) incoming beams. The results are qualitatively independent of the specific breather wave in the system; for simplicity and without loss of generality we launch a two-soliton breather with oscillation period $Z_T=\frac{2\pi}{8}$ [30]:

$$\psi(X,Z_0) = \frac{4[\cosh 3X + 3\cosh X \exp i(8Z_0)]}{\cosh 4X + 4\cosh 2X + 3\cos(8Z_0)}. \tag{10}$$

The emerging wave ψ_+ is then

$$\psi_+ = |P(X,Z_0)|\exp i[\delta|P(X,Z_0)|^2 + S(X,Z_0)] \tag{11}$$

with

$$|P(X,Z_0)|^2 = \frac{16[9\cosh^2 X + 6\cos(8Z_0)\cosh X\cosh 3X + \cosh^2 3X]}{[3\cos(8Z_0) + 4\cosh 2X + \cosh 4X]^2},$$

$$S(X,Z_0) = \arctan\left(\frac{3\cosh X\sin(8Z_0)}{3\cos(8Z_0)\cosh X + \cosh 3X}\right),$$

$$P_0(Z_0)^2 = \frac{32}{5 + 3\cos(8Z_0)} \tag{12}$$

with $|P(X,Z_0)|\leqslant P_0(Z_0)$. When $\delta|P(X,Z_0)|^2$ and $S(X,Z_0)$ have curvatures in X of different signs, the chirp content (i.e., the second derivative in X) of $\delta|P(X,Z_0)|^2$ needs first to balance the opposite curvature of $S(X,Z_0)$ and (significantly) alter the overall phase in order to destabilize the system. Therefore, we do not expect soliton splitting for small δ (at least in a perturbative regime). When the curvatures of $\delta|P|^2$ and S are of the same sign, conversely, we can apply our asymptotic expansion using $\epsilon=P_0^{-1}$ and obtain the critical δ_c^* (Fig. 2, dotted line):

$$\delta_c = \begin{cases} \delta_c^*(Z_0), & 0\leqslant Z\leqslant Z_T/2, \\ -\delta_c^*(-Z_0), & Z_T/2\leqslant Z\leqslant Z_T, \end{cases}$$

$$\delta_c^* = \frac{\sqrt{2}[5 + 3\cos(8Z_0)]}{8\sqrt{23 - 15\cos(8Z_0)}} + \frac{1}{[23 - 15\cos(8Z_0)]^2}\left(\frac{9}{16}\sin(16Z_0) + \frac{135}{64}\sin(24Z_0) - \frac{1245}{64}\sin(8Z_0)\right). \tag{13}$$

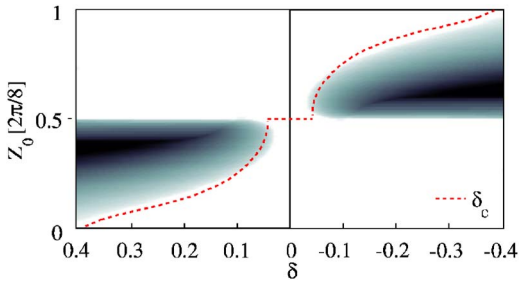

FIG. 2. (Color online) Calculated real part of the largest imaginary eigenvalue (pseudocolor plot) and predicted critical chirp δ_c (dotted line) versus defect displacement Z_0 and strength δ.

To verify our predictions, we numerically solve the ZS problem versus strength δ and position Z_0 of the nonlinear defect [Fig. 2, pseudocolor plot]. As apparent, numerical and predicted δ_c match well and no soliton splitting is observed for curvatures of different signs; a significant reduction of δ_c is achieved for Z_0 close to the amplitude peaks of the breathing wave. It is noteworthy that, even for parameters beyond the range where the perturbative expansion is valid [i.e., for $\delta > O(\epsilon)$], the numerics confirm the phenomenology we previously addressed theoretically, with an increased transverse velocity after splitting. We therefore underline this feature: the onset of soliton emission can be adjusted. The latter effect can also take place by tuning the power for a fixed Z_0 in a region where the excitation exhibits (intensity-dependent) oscillations. Since this occurs for specific input powers N, it allows a complete (nonlinear) control over the phenomenon. To elucidate such type of response, we exploit the dynamics of a high-order soliton $\psi(X,0)=\sqrt{N}\mathrm{sech}\, X$, with $1 \leqslant N < 4$. In fact, the single-soliton long-time behavior for $R(Z)=0$ is approached after an oscillating transient with period adiabatically changing from ∞ ($N=1$) to Z_T ($N \to 4$) [30]. For instance, taking $Z_0=0.6$ and $\delta=0.26$, we solve Eq. (2) versus excitation N with the aid of a beam propagation code (Fig. 3). As foreseen, the solitary breather splits immediately before the oscillation peak comes close to the defect in Z_0 (Fig. 3, dotted line), while no symmetry breaking is observed for $N>3$ (due to the sign change in the phase curvature of ψ) in perfect agreement with our model. Hence, the excitation N precisely determines the system outcome for a given defect position Z_0, thus permitting all-optical soliton emission at a longitudinal nonlinear defect.

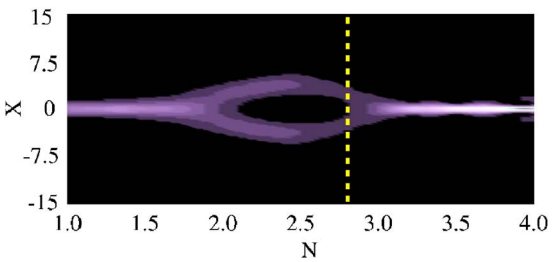

FIG. 3. (Color online) (Pseudocolor plot) output intensity sections after a distance $Z=Z_0+L=3Z_T+Z_0$ versus input power N (for $Z_0=0.6$ and $\delta=0.26$); (dotted line) oscillation peak crossing Z_0.

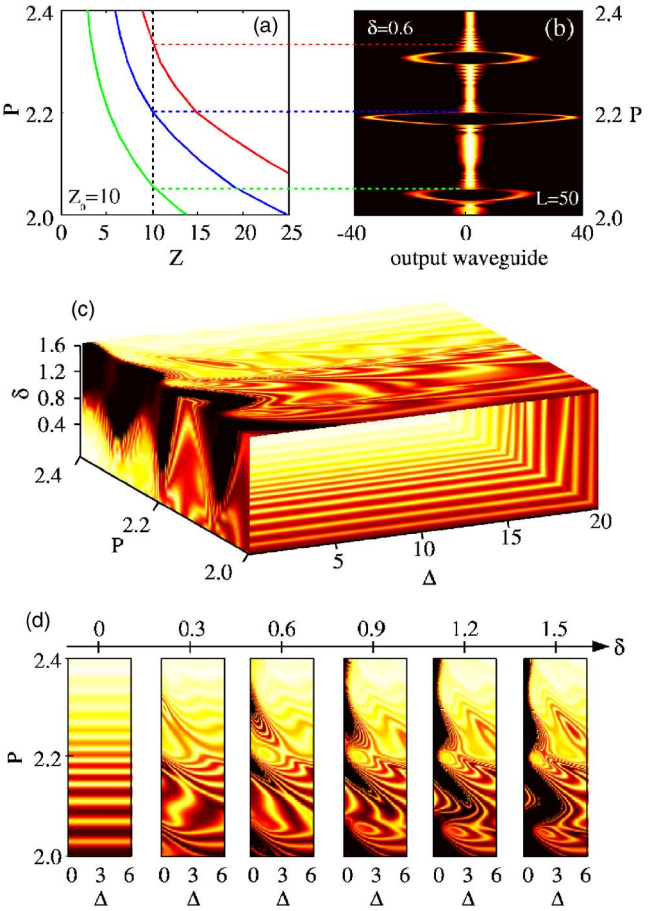

FIG. 4. (Color online). (a) Z position of the first three oscillation peaks versus input power P (for $Z_0=10$ and $\delta=0.6$); (b) output intensity distribution in $Z=Z_0+L=60$ versus input power P; (c) output intensity sections in $X=0$, versus input power P, defect length Δ, and defect strength δ; (d) sections of (c) at specific δ.

B. Dynamics at extended defects

When Δ is much greater than any characteristic soliton length, the defect takes the expression $R(Z)=\frac{\delta}{2}u_{-1}(Z-Z_0)$, with $u_{-1}(Z)$ the Heaviside function. It is convenient to rescale Eq. (2) into a dissipative form:

$$i\frac{\partial\psi}{\partial Z}+\frac{\partial^2\psi}{\partial X^2}+2|\psi|^2\psi=i\beta(Z)\psi, \tag{14}$$

having introduced $\psi=\phi\exp(-\Gamma)$, $\Gamma=\int\beta(Z)dZ$, and $\beta=\frac{\ln(1+\delta/2)}{2}u_0(Z-Z_0)$. In this case the emerging beam $\psi_+=\psi_-\exp(\frac{\ln 1+\delta/2}{2})$ is a scaled replica of the incoming wave ψ_- and, therefore, it evolves towards a soliton with a higher energy (assuming positive δ). No splitting is expected.

III. LATTICE SIMULATIONS

Based on the theoretical model discussed above, a rich splitting scenario is offered by the interaction of an immobile defect $R(Z)$ with a localized or solitary wave with a breathing character (at least over the initial propagation distance in front of the defect) for $\Delta \ll 1$. For the most "discrete" situa-

tion, we exploit the dynamics of a simple Kronecker input $q_n(0)=A\delta_{n0}$. For the simulations we used an array of 300 waveguides and a step-adaptive algorithm. When the power $P=A^2$ overcomes discrete diffraction, the system approaches a stable state by a breathing transient with both period and peak-to-peak amplitude adiabatically reducing to zero as $P \to \infty$ (i.e., when the discrete soliton extends over a single channel waveguide) [see Fig. 4(a) for $Z_0=10$]. For small δ, we expect the breathing input to break into two solitons immediately before its oscillation peak reaches the defect in Z_0. This is visible in Fig. 4(b) as the first three peaks move close to Z_0 for $P \approx 2.0$, 2.2, and 2.35, respectively (owing to the small $\delta=0.6$, no other breaking is observed). The latter scenario completely changes for $\Delta \gg 1$, when no splitting is expected. To investigate the transition between the limits $\Delta \ll 1$ and $\Delta \gg 1$, and therefore provide a connection with the previous theoretical analysis, we numerically acquired the output intensity in $X=0$ versus excitation and defect parameters δ, Δ [Figs. 4(c) and 4(d)]. As Δ increases, the splitting regions adiabatically shrink in power and move downward (due to intensity gain in the defect), eventually overlapping for large Δ. For higher Δ the system moves to a region where no emission takes places, in agreement with the previous analysis. These findings suggest that a proper combination of defects with different size could precisely control the power intervals for soliton splitting, with potential applications in wavelength filters and/or demultiplexers. As the coupling between evanescently coupled waveguides is quite sensitive to wavelength (much more than in bulk media), nonlinear splitting could generate solitons with differing directions of propagation at each wavelength; conversely, for a narrow splitting region in power, only a few wavelengths could be filtered out from the whole incoming spectrum. Optically controlled switches, logic gates, and diodes (the effect is nonreciprocal [36]) can be envisioned, as well as power filters to be employed in feedback systems with mono- or bistable response.

Among various suitable discrete systems, nematic liquid crystalline arrays offer electro-optic tunability and a large optical nonlinearity [7,37]. An electric field (at low or optical frequency) exerts a torque on the elongated NLC molecules, which change orientation (hence increase the extraordinary index of refraction) until a balance is reached with the (intermolecular) elastic forces [38]. The nonlinear response associated with light-induced reorientation can be further tuned (enhanced, reduced, or even reversed) by doping the NLC with azo-dye compounds, as an additional photoinduced torque arises from a guest (dye)–host (NLC) interaction [39,40]. This nonlinear contribution can be controlled by acting on the polarization and/or intensity of an external illumination [41], allowing on-site direct all-optical control of a nonlinear defect with prescribed and adjustable strength and size at a specific location of the array.

In conclusion, we have developed a detailed model of discrete nonlinear light dynamics in the presence of a single longitudinal nonlinear defect of arbitrary amplitude, position, and strength. The underlying physics permits to gain full control over the system. We anticipate a series of applications as well as an entirely different approach to soliton-based data processing, where interactions are exploited by all-optically acting on nonlinearity. We envision these concepts to be readily exploited in azo-dye-doped liquid crystalline 1D arrays, as well as in other light-manageable lattices.

ACKNOWLEDGMENTS

We thank C. Conti and D. Levi for useful discussions.

[1] H. Feddersen, Phys. Lett. A **154**, 391 (1991).
[2] D. N. Christodoulides and R. I. Joseph, Opt. Lett. **13**, 794 (1988).
[3] A. Trombettoni and A. Smerzi, Phys. Rev. Lett. **86**, 2353 (2001).
[4] A. J. Sievers and S. Takeno, Phys. Rev. Lett. **61**, 970 (1988).
[5] D. N. Christodoulides, F. Lederer, and Y. Silberberg, Nature (London) **424**, 817 (2003).
[6] J. W. Fleischer, M. Segev, N. K. Efremidis, and D. N. Christodoulides, Nature (London) **422**, 147 (2003).
[7] A. Fratalocchi, G. Assanto, K. A. Brzdakiewicz, and M. A. Karpierz, Opt. Express **13**, 1808 (2005).
[8] A. Anderson and M. A. Kasevich, Science **282**, 1686 (2001).
[9] F. K. Abdullaev, E. N. Tsoy, B. A. Malomed, and R. A. Kraenkel, Phys. Rev. A **68**, 053606 (2003).
[10] D. N. Christodoulides and E. D. Eugenieva, Phys. Rev. Lett. **87**, 233901 (2001).
[11] V. V. Konotop, D. Cai, M. Salerno, A. R. Bishop, and N. Gronbech-Jensen, Phys. Rev. E **53**, 6476 (1996).
[12] A. Trombettoni, A. Smerzi, and A. R. Bishop, Phys. Rev. E **67**, 016607 (2003).
[13] S. Burtsev, D. J. Kaup, and B. A. Malomed, Phys. Rev. E **52**, 4474 (1995).
[14] I. Bena, A. Saxena, and J. M. Sancho, Phys. Rev. E **66**, 036617 (2002).
[15] W. C. K. Mak, B. A. Malomed, and P. L. Chu, Phys. Rev. E **67**, 026608 (2003).
[16] R. H. Goodman, P. J. Holmes, and M. I. Weinstein, Physica D **192**, 215 (2004).
[17] G. B. Whitham, *Linear and Nonlinear Waves* (Wiley, New York, 1999).
[18] U. Peschel and F. Lederer, J. Opt. Soc. Am. B **19**, 544 (2002).
[19] B. A. Malomed, D. F. Parker, and N. F. Smyth, Phys. Rev. E **48**, 1418 (1993).
[20] J. Cuevas, B. A. Malomed, and P. G. Kevrekidis, Phys. Rev. E **71**, 066614 (2005).
[21] Y. Gaididei, N. Flytzanis, A. Neuper, and F. G. Mertens, Phys. Rev. Lett. **75**, 2240 (1995).
[22] B. Maune, M. Loncar, J. Witzens, M. Hochberg, T. B. Jones, D. Psaltis, A. Scherer, and Y. Qiu, Appl. Phys. Lett. **85**, 360 (2004).
[23] K. Busch and S. John, Phys. Rev. Lett. **83**, 967 (1999).
[24] S. W. Leonard, J. P. Mondia, H. M. van Driel, O. Toader, S. John, K. Busch, A. Birner, U. Gosele, and V. Lehmann, Phys.

Rev. B **61**, R2389 (2000).
[25] P. G. Kevrekedis, K. O. Rasmusses, and R. Bishop, Int. J. Mod. Phys. B **15**, 2833 (2001).
[26] A. B. Aceves, C. De Angelis, T. Peschel, R. Muschall, F. Lederer, S. Trillo, and S. Wabnitz, Phys. Rev. E **53**, 1172 (1996).
[27] A. C. Newell, *Solitons in Mathematics and Physics* (SIAM, Philadelphia, 1985).
[28] A. Jeffrey and T. Kawahara, *Asymptotic Methods in Nonlinear Wave Theory* (Pitman, Boston, 1982).
[29] M. J. Ablowitz, B. Prinari, and A. D. Trubatch, *Discrete and Continuous Nonlinear Schrödinger Systems* (Cambridge University Press, Cambridge, U.K., 2004).
[30] J. Satsuma and N. Yajima, Suppl. Prog. Theor. Phys. **55**, 284 (1974).
[31] J. C. Bronski, Physica D **97**, 376 (1996).
[32] J. J. Sakurai, *Modern Quantum Mechanics* (John Wiley & Sons, New York, 1994).
[33] T. Poston and I. Stewart, *Catastrophe Theory and Its Applications* (Dover, New York, 1978).
[34] R. Gilmore, *Catastrophe Theory for Scientists and Engineers* (Dover, New York, 1981).
[35] E. Ott, *Chaos in Dynamical Systems* (Cambridge University Press, Cambridge, U.K., 1997).
[36] K. Gallo, G. Assanto, K. R. Parameswaran, and M. M. Fejer, Appl. Phys. Lett. **79**, 314 (2001).
[37] A. Fratalocchi and G. Assanto, Phys. Rev. E **72**, 066608 (2005).
[38] I. C. Khoo, *Liquid Crystals: Physical Properties and Nonlinear Optical Phenomena* (Wiley, New York, 1995).
[39] I. Jánossy and L. Szabados, Phys. Rev. E **58**, 4598 (1998).
[40] M. Becchi, I. Jánossy, D. S. Shankar Rao, and D. Statman, Phys. Rev. E **69**, 051707 (2004).
[41] A. Pasquazi, A. Alberucci, M. Peccianti, and G. Assanto, Appl. Phys. Lett. **87**, 261104 (2005).